A&A 374, 454–464 (2001)
DOI: 10.1051/0004-6361:20010750

Astronomy & Astrophysics

ROSAT-HRI observations of six southern galaxy pairs

G. Trinchieri and R. Rampazzo

Osservatorio Astronomico di Brera, via Brera 28, 20121 Milano, Italy

Received 3 April 2001 / Accepted 25 May 2001

Abstract. We present the detailed analysis of the X–ray data for 6 pairs, isolated or in poor groups, observed at high resolution with the ROSAT HRI . In all cases, the stronger X–ray source is associated with the brighter early-type member and is extended. The extent varies from galactic to group scale, from 3 (RR 210b) to 182 kpc(RR 22a). The fainter members are detected only in two pairs, RR 210 and RR 259. Except for one case, no significant substructures have been detected in the X–ray maps, possibly also as a consequence of the poor statistics. The core radii of the X–ray surface brightness profiles are in the range 1–3 kpc. The distribution of the luminosities of galaxies in pairs encompasses a very wide range of both luminosities and L_X/L_B ratios, in spite of the very small number of objects studied so far. Our data provide no evidence that pair membership affects the X–ray properties of galaxies. Observation are discussed in the context of the pair/group evolution.

Key words. galaxies: individual: general – galaxies: interactions – X–rays: galaxies

1. Introduction

Pairs of galaxies with elliptical members and isolated ellipticals in the field could represent different phases in the coalescence process of groups (e.g. Rampazzo & Sulentic 1992; Mulchaey & Zabludoff 1999). The study of pair properties could be then deeply interconnected with that of groups. In particular their X–ray properties could be useful in addressing the question of the origin and fate of the hot Intra-Group Medium (IGM), often found in poor groups of galaxies (see e.g. Mulchaey et al. 1993; Pildis 1995; Mulchaey et al. 1996; Ponman et al. 1996; Mulchaey & Zabludoff 1998: MZ98 hereafter; Helsdon & Ponman 2000).

The IGM in groups is cooler than in clusters ($kT \approx 1$–2 keV) and not as luminous nor as extended, and possibly it has a closer connection with the dominant central galaxy than in clusters. MZ98 analyzed the X–ray data of 12 poor groups and found that in most cases the X–ray emission is centered on a luminous elliptical galaxy. The surface brightness profiles of the X–ray emission suggest the presence of two X–ray components. One, probably associated with the galaxy itself, has a scale of 40–80 kpc ($H_0 = 50$ km s^{-1} Mpc^{-1}). The second is detected out to a radius of 200–600 kpc and its properties fit well in the relationships found among the X–ray temperature, X–ray luminosity and optical velocity dispersion of rich clusters. The authors suggest that this latter component could represent a low mass version of the Intra-Cluster Medium.

Send offprint requests to: G. Trinchieri,
e-mail: ginevra@brera.mi.astro.it

Since the number of poor groups studied is increasing, attempts at classifying them into an evolutionary sequence combining their X–ray properties to galaxy population (presence of satellite galaxies, ratio between early and late type galaxies, etc.) and group dynamical information are developing.

Zabludoff (1999) suggests that groups could fall into different classes defined by their X–ray properties. Groups with extended, hot IGM also have the giant elliptical, typically the brightest group galaxy, that lies near or on the peak of the "smooth, symmetric" X–ray emission. Most of the poor groups studied by MZ98 would fall in this class. Groups without X–ray emission would consist of a few bright late-type galaxies and their satellites, not very different from the Local Group. If the group evolution is such that systems dominated by late–type objects could evolve into groups dominated by a central, giant elliptical and a detectable IGM, transition systems could form a third class of objects. These "evolving groups" would clearly show signatures of the recent dynamical evolution in their cores, including interacting galaxies, and any extended X–ray emission would not be smooth and regular, and would not be associated with single galaxies. In this context, the X–ray properties of NGC 2300 (Mulchaey et al. 1993) would classify it among the poor groups with extended hot IGM. Optically, however, the "group" is formed by a very small number of galaxies, a dominating interacting pair formed by an elliptical (NGC 2300) and a spiral (NGC 2276) plus two lower luminosity satellite galaxies. This suggests that mixed morphology (and early type) pairs of galaxies could be a reasonable system in which to

Table 1. Log-book of the observations.

Object	Obs. Dates Beginning - End	On Time s	PI
RR 22	28/12/97–30/12/98	23 098	S. Döbereiner
RR 143	26/03/96–06/04/96	16 850	J. Beuing
	04/08/96–17/08/96	11 686	
RR 210	19/06/97–27/06/97	81 143	G. Trinchieri
RR 216	06/01/97–11/0197	47 655	G. Trinchieri
	27/06/97–03/08/97	15 735	
	10/01/98–21/01/98	24 702	
RR 242	30/01/96–04/02/96	12 293	J. Beuing
RR 259	06/02/96–10/02/96	15 994	T. Hawarden
	25/07/96–28/07/96	40 776	

investigate both the evolution of galaxy groups and the question concerning the origin and fate of the gas heated by the large energy input from stellar evolution, possibly triggered by interaction.

In this context, the analysis of the X–ray emission from 52 pairs in the *Catalogue of Isolated Pairs of Galaxies* (CPG: Karachentsev 1987 and reference therein) by Henriksen & Cousineau (1999: HC99) did not find that the X–ray properties of pairs are similar to those of groups; with one remarkable exception (CPG 564), the extension of the X–ray emission is ≈10–50 kpc, i.e. much smaller than expected for group intergalactic medium, and likely originating from galaxies. They claim that the luminosity of these objects is also lower relative to "single" galaxies of the same optical luminosity.

We contribute to the discussion with the detailed analysis of ROSAT HRI data for 6 interacting pairs of galaxies (see Table 1) selected from the catalog of Reduzzi & Rampazzo (1995: R&R95 hereafter). Candidate pairs have been selected from the ESO-LV catalog (Lauberts & Valentijn 1989), complete to $m_B = 14.5$ mag, using isolation criteria similar to those applied by Karachentsev (1987) for the CPG, which are based on galaxy separation and diameters, since the redshift was not available for a significant fraction of the galaxies. Up to now redshifts are available for 59% of the candidates. Some of the basic (mostly optical) characteristics of the objects presented here are summarized in Table 2 and are discussed in Sect. 2. The sample is very small, and probably very biased (toward more famous and better studied objects), nevertheless it appears to provide enough information that some general conclusions can be drawn from it, as will become clear in the discussion. A value of $H_0 = 50$ km s^{-1} Mpc^{-1} is used for all calculated quantities.

2. The sample

2.1. The sample selection

We have selected pairs from the R&R95 catalog that fall within a ROSAT-HRI pointed observation, that are observed near the field's center and long enough so that we can perform a morphological study of their emission, to study their characteristics in some detail. Most of the galaxies have not previously appeared in the literature, so we present the details of the data analysis in the next section. RR 75 (NGC 1316 or Fornax A and NGC 1317), RR 206, the Antennae (NGC 4038/NGC 4039) and RR 368 (the central interacting pair in HCG 91) are also selected according to the above criteria, but have already been exhaustively presented in the literature (Fabbiano et al. 1997; Ponman et al. 1996; Kim et al. 1998) and we would use the results where appropriate. However, we notice that only RR 75 is relevant to this study, since the emission from the other two objects, though extremely interesting, is dominated by the emission from a Seyfert galaxy in the group (RR 368, Ponman et al. 1996) or by the effects of the ongoing merging of gas rich galaxies, that directly produces many bright individual sources and more extended diffuse emission (RR 206, Fabbiano et al. 1997).

2.2. Notes on individual objects

RR 22, NGC 439/NGC 441. NGC 439/NGC 441 are by far far the two brightest members of a group, which includes several other fainter satellites. In their analysis of the environmental properties of luminous galaxies, that includes NGC 439, Cappi et al. (1998) show that this kind of galaxy is easily clustered and that a large fraction of such galaxies are in interacting pairs, show tidal distortions or appear to be surrounded by satellite galaxies. The size of the group is uncertain: Maia et al. (1989) attribute 7 members to it (group #61), while Ramella et al. (1996) count 18 members with a velocity dispersion of 283 ± 39 km s^{-1}.

Carollo & Danziger (1994) studied NGC 439 in detail, and found no significant peculiarities either in the photometry or in the kinematics. The rotation velocity along the major axis has an amplitude of ≈50 km s^{-1} and no rotation is detected along the minor axis.

RR 143, NGC 2305/NGC 2307, AM0648-641. The pair appears truly isolated but has a rather large ΔV (see Table 2). The photometric study by Reduzzi & Rampazzo (1996: R&R96 hereafter) shows that RR 143a is an elliptical with some sub-structures visible both in the ellipticity and in the isophotal shape profile, while RR 143b has a well developed bar, frequently found in interacting spirals (Elmegreen & Elmegreen 1982; R&R96), and its arm structure is grand design. The color profiles are typical of the morphological class of each component. The bar shows a uniform color $(B-V) \approx 1$ quite red with respect to the rest of the galaxy suggestive of an old stellar population.

In spite of the high ΔV, we tentatively consider this a physical pair, since examples of pairs that can be modeled

Table 2. Basic properties of the pair members and of the pairs.

galaxy	RR 22a	RR 22b	RR 143a	RR 143b	RR 210a	RR 210b
data	NGC 439	NGC 441	NGC 2305	NGC 2307	NGC 4105	NGC 4106
ESO number	4 120 180	4 120 190	870 440	870 450	4 400 540	4 400 560
Type	−3.8	−0.3	−5.0	3.0	−4.0	−2.0
RA (2000)	01 13 47	01 13 51	06 48 36	06 48 50	12 06 41	12 06 45
Decl. (2000)	−31 44 51	−31 47 15	−64 16 24	−64 20 01	−29 45 42	−29 46 06
Hel. Vel. (km s^{-1})	5769	5688	3522	4589	$1912 * \pm 23$	$2170 * \pm 18$
$\langle\sigma_0\rangle$ (km s^{-1})	300 ± 25		215 ± 20		$277 * \pm 22$	$253 * \pm 17$
a_{25} (arcsec)	188.4	92.3	134.9	110.9	221.3	237.1
B	12.38	13.76	12.82	13.38	11.35	11.61
$(B-R)$	1.57	1.58	1.84	1.62	1.82	
IRAS $S_{12\mu}$	0 ± 26		0 ± 27		0 ± 21	0 ± 21
IRAS $S_{25\mu}$	0 ± 39		0 ± 22		0 ± 36	0 ± 27
IRAS $S_{60\mu}$	0 ± 46		0 ± 40		270 ± 40	230 ± 22
IRAS $S_{100\mu}$	0 ± 97		0 ± 91		740 ± 135	630 ± 151
pair data	RR 22		RR 143		RR 210	
Proj. sep. (arcsec)	153		234		59	
ΔV (km s^{-1})	81		1036		258	
$N_{\rm tot}$	12.0		3.501		4.138	
Distance (Mpc)	114		81		40	

galaxy	RR 216a	RR 216b	RR 242a	RR 242b	RR 259a	RR 259b
data	IC 3290	NGC 4373	NGC 5090	NGC 5091		NGC 5291
ESO number	3 220 040	3 220 060	2 700 020	2 700 040	4 450 300	4 450 301
Type	−0.5	−3.0	−5.0	3.0	2.0	−2.0
RA (2000)	12 25 09	12 25 18	13 21 12	13 21 18	13 47 23	13 47 25
Decl. (2000)	−39 46 31	−39 45 37	−43 42 16	−43 43 10	−30 24 25	−30 23 49
Hel. Vel. (km s^{-1})	3342	3415	3421	3529	4386	4396
$\langle\sigma_0\rangle$ (km s^{-1})		234 ± 23	272 ± 27			
a_{25} (arcsec)		275.4	162.2	120.2	53.7	75.0
B	12.97	11.59	12.59	13.94	15.18	14.09
$(B-R)$	1.54	1.50	1.75	1.51	1.61	1.70
IRAS $S_{12\mu}$		0 ± 25	110 ± 29			0 ± 30
IRAS $S_{25\mu}$		0 ± 45	190 ± 26			0 ± 41
IRAS $S_{60\mu}$		0 ± 45	170 ± 46			0 ± 52
IRAS $S_{100\mu}$		0 ± 169	760 ± 397			0 ± 92
pair data	RR 216		RR 242		RR 259	
Proj. sep. (arcsec)	118		77		41	
ΔV (km s^{-1})	73		108		10	
$N_{\rm tot}$	15.50		1.910		15.167	
Distance (Mpc)	67		69		87	

Notes: Galaxy data (morphological type, coordinates, heliocentric velocity, diameter at $\mu_B = 25$ mag arcsec^{-2}, total apparent B mag and $(B-R)$ color) are from ESO-LV. The average values of central velocity dispersion, $\langle\sigma_0\rangle$, are from the "Hypercat Catalog" available on line at `http://www-obs.univ-lyon1.fr/hypercat/` except those with an asterisk, that are from Longhetti et al. (1998). IRAS data are from Knapp et al. (1989). Pair data are from R&R95. $N_{\rm tot}$ gives the number of galaxies per square degree (see ESO-LV). Distances are calculated from the systemic velocity assuming $H_0 = 50$ km s^{-1} Mpc^{-1}.

as high velocity, unbound encounters have appeared in the literature (see e.g. Combes et al. 1995). Although these models focus on E+E morphology, we cannot exclude a high velocity and/or unbound encounter for RR 143 at this stage.

RR 210 (NGC 4105/NGC 4106, AM1204-292). Information from the literature is quite contradictory. In the Arp & Madore (1987) catalogue, the object is classified as a pair. Tully (1988) associates NGC 4105 and NGC 4106 to IC 764, i.e. a triplet. In fact, although quite separated in projection from NGC 4105/4106, the heliocentric velocity of IC 764 (2127 ± 14 km s^{-1}: ESO-LV) is consistent with the systemic velocity of the pair. Garcia (1993) instead assigns NGC 4105 and NGC 4106 to

separate groups, LGG 270 and LGG 271 respectively, defined by his "algorithm" applied to the catalog of 78 000 objects of the Lyon-Meudon Extragalactic Database.

R&R96 present the B, V and R surface photometry for the pair, and suggest that both members are early-type galaxies (see Table 2). RR 210a is disc-like in the outskirts (however, light contamination by the companion is strong), and becomes box-like in the inner 50″, with dust in the center. RR 210b is instead disc-like all the way to the center. The $(B-V)$ color profiles of both galaxies are ≈1, consistent with their morphological classification. The diffuse, rounded arms/tails visible in RR 210b are most likely generated by the on-going interaction (see e.g. the simulations by Noguchi 1990). Both galaxies are far-IR sources (see Table 2 and Knapp et al. 1989).

Longhetti et al. (1998) obtained the kinematic and spectro-photometric properties of both galaxies. The distorted velocity and velocity dispersion profiles of RR 210a obtained along the line connecting the two nuclei suggest that the two objects are strongly interacting. [O II] λ 3727 Å emission line has been detected in the nucleus. The study of the line strength indexes presented in Longhetti et al. (1998) and in Longhetti et al. (2000) suggests the presence of very recent star formation episodes. RR 210b in particular shows a value of the index H + K(CaII) > 1.3, i.e. larger than the maximum value attainable in post-star-burst models (both with solar and non solar metallicity), suggesting the presence of Hϵ in emission. This feature is considered a good indicator of star formation (Rose 1984, 1985).

RR 216, IC 3290/NGC 4373, AM1222–392. This system is a pair also according to Sadler & Sharp (1984) and Arp & Madore (1987). Both galaxies are in the Hydra-Centaurus region (see Dickens et al. 1986; Garcia 1993) but located at the outskirts, at 4.9 degree (5.7 Mpc) from the cluster center (Dickens et al. 1986).

From the B, V, R surface photometry, R&R96 derive $(B-V)$ color ≈1 throughout the galaxy for both objects, which suggests that they are both early-types and that the spiral structure is probably generated by the interaction (see Noguchi 1990). Dust features are detected in NGC 4373.

RR 242, NGC 5090/NGC 5091. This is a typical E+S pair. NGC 5090 (PKS B1318-434) has two large-scale radio jets (see Lloyd et al. 1996 and reference therein) with the radio axis perpendicular to the line connecting the nuclei of the pair members. This has suggested that the tidal interaction may be influencing the way in which the central engine of the elliptical is fueled.

Carollo et al. (1993) have obtained the velocity dispersion and rotation velocity profiles of NGC 5090. Its apparent major axis is positioned at 110° but the galaxy has been observed along the axes at 270° and 360°. The central velocity dispersion peaks around 300 km s^{-1} and the observed amplitude of the rotation curve is between 50 and 75 km s^{-1}, indicating that the galaxy is a typical elliptical galaxy as classified in the ESO-LV catalogue.

RR 259, /NGC 5291. According to the classification in ESO-LV the pair is composed of an early-type, NGC 5291 and a late-type galaxy, the so called "sea-shell" galaxy. NGC 5291 is a LINER (Duc & Mirabel 1997). The pair, located at the edge of the Abell 3574 cluster, shows various signatures of ongoing interaction. A large quantity of atomic gas (≈5×10^{10} $M_\odot$) forms a sort of fragmented ring, probably the debris of past episodes of interaction. The ring seems to host Tidal Dwarf Galaxy candidates (Duc & Mirabel 1998).

In spite of the selection criteria, RR 22 is in a group. RR 216 and RR 259 are at the edge of richer environments, so that they might not be truly isolated, while all others are in poor environments. However, the observed signatures of ongoing gravitational interaction between the two members, and/or the low systemic velocity differences, are strong signs of truly interacting pairs.

3. Results of the ROSAT data analysis

All pairs were observed with the HRI near the field center (the most off-center, RR 259, is ≈7′ off-axis) (for a full description of the ROSAT satellite and of the instrument, see Trümper 1983; Trümper et al. 1991; Zombeck et al. 1995). As described in Table 1, two observations (RR 210 and RR 216) were obtained in AO7 by us, all others have been extracted from the ROSAT archive. We have used the images produced by the standard automatic processing. The observation of RR 216 was split in 3 separate segments. However, since the pointing is the same, we have simply added all data together and have worked on the resulting merged image. The data analysis was done mostly with the *xray* package in `IRAF`. The "csmooth" routine in the CIAO2 software package was also used to produce adaptively smoothed images.

Figure 1 presents the iso-contours of the smoothed X–ray images overlayed onto the Digitized Sky Survey plates[1] for the galaxies studied here. A detection of the brightest member is obtained in all cases. Both members are detected in RR 210 and RR 259.

To produce the X–ray maps and to study the overall morphological characteristics of these galaxies, we have selected Pulse Height Analyzer (PHA) channels 1–10, to improve on the signal-to-noise (Trinchieri & Pietsch 1900, see also the discussion on the HRI background in "The ROSAT High Resolution Imager (HRI) Calibration Report"[2]). The field background is to first approximation flat, the effects of vignetting being rather small in the PHA channel range chosen and in the inner 10′ radius region, so we could choose the background in a region in

[1] The Digitized Sky Survey was produced at the Space Telescope Science Institute (STScI) under U.S. Government grant NAG W-2166.

[2] Available on line at
`http://hea-www.harvard.edu/rosat/rsdc_www/hricalrep.html`

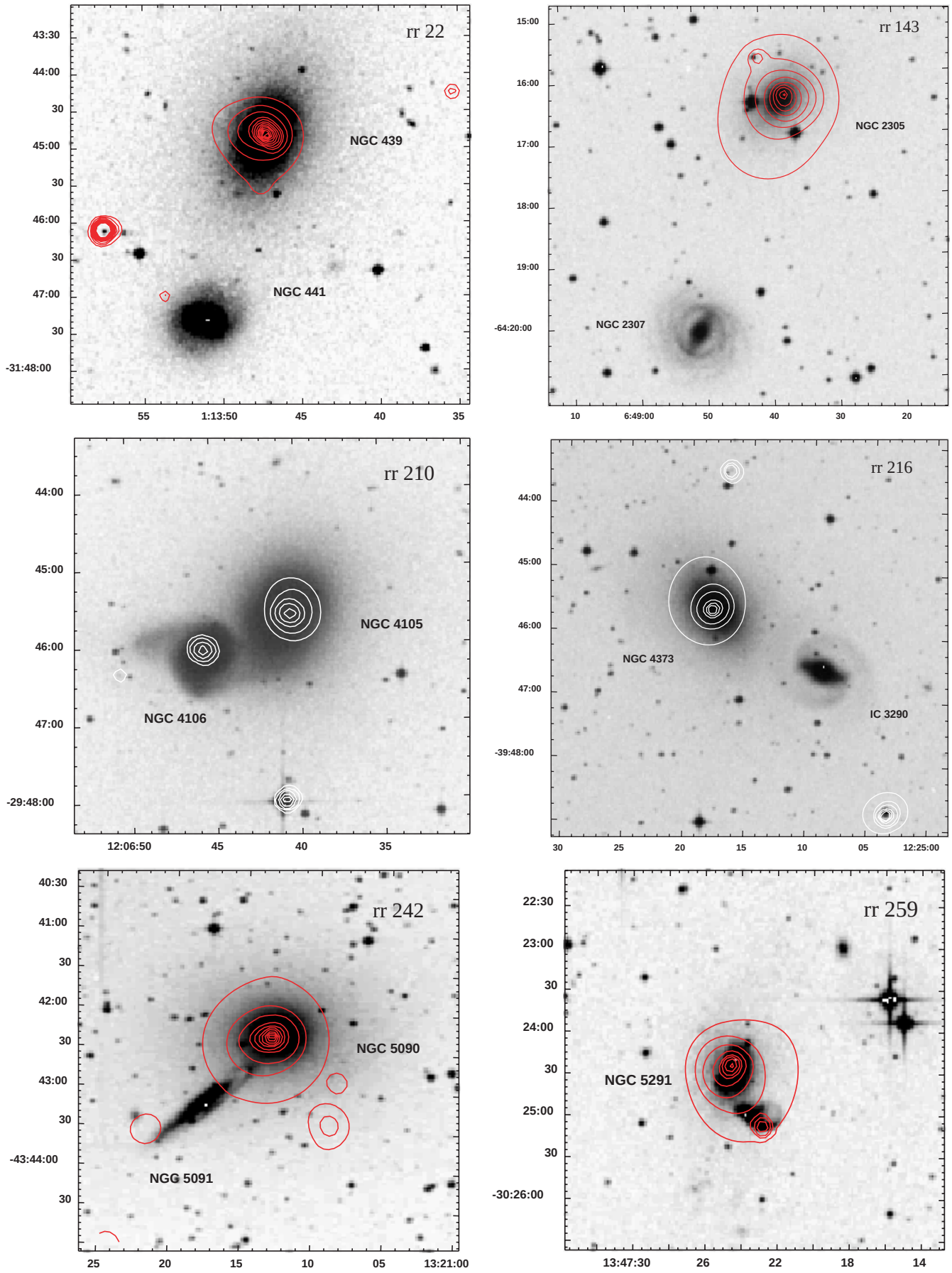

Fig. 1. Iso-intensity contour plot of the X–ray emission of all pairs superposed on the DSS images. The data have been smoothed with an adaptive filter (see text).

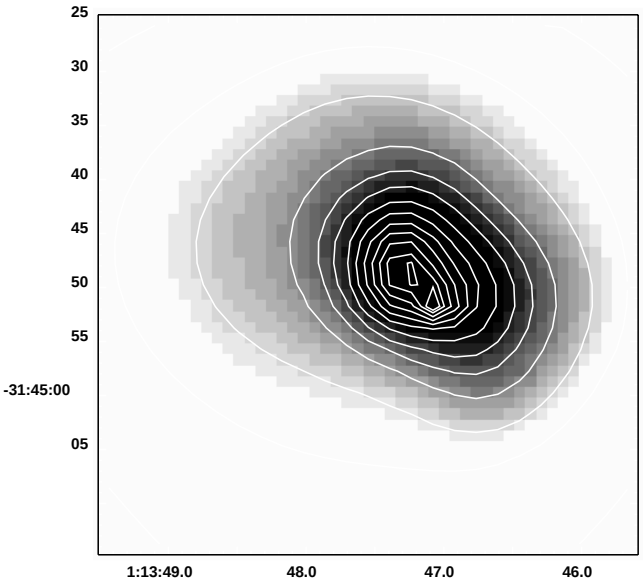

Fig. 2. Adaptive smoothing of the inner region of RR 22.

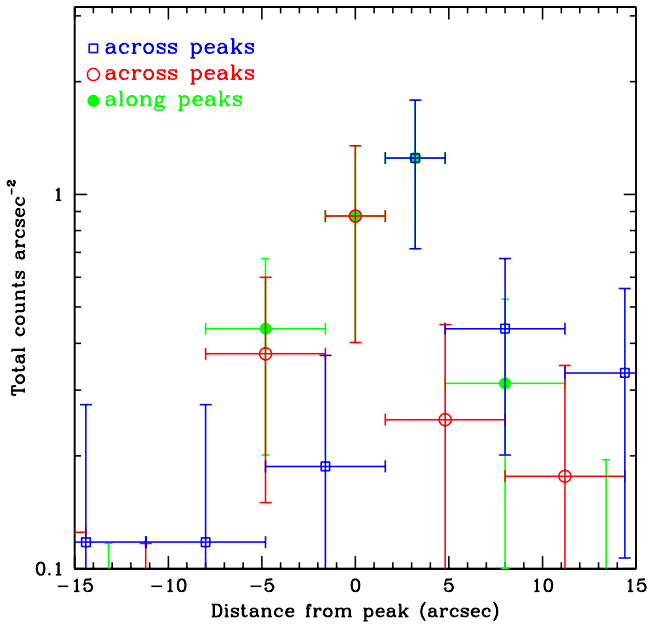

Fig. 3. Distribution of the total counts in RR 22 along PA = 50°, crossing the two peaks (Solid symbols), and along the perpendicular direction, centered on the NE (open circles) and SW (boxes) peaks.

the same field, outside the emission associated with the targets. The PHA range chosen should also ensure that the inhomogeneities in the background due to changes in gain across the detector should not be severe. We have typically chosen the background in an annulus around the sources. For RR 259, ∼7′ off-axis, we have chosen an annulus centered at the field's center, at a similar off-axis as RR 259, with the exclusion of a 7′ circle centered on the X–ray source. The background levels assumed have also been checked against the expected background obtained from a few fields relatively empty of sources.

The large scale photon spatial distribution is regular in most galaxies. The small azimuthal asymmetries visible in the images of RR 22 and RR 143 are confirmed by the analysis of the photon distribution in different angular sectors. In particular, the emission in RR 22 is slightly elongated along PA ∼ 50°. The excess to the N seen in RR 143, in the 0.6′−1′ annulus, appears to be associated to a background source, and we have therefore excluded it from the radial profile. At the center, only RR 22 (Fig. 2) shows a peculiar photon distribution, with contours elongated towards the SW, and a possible bend towards the south, where a second sharp peak is located. Cuts along the two peaks and across it, shown in Fig. 3, confirm the visual impression from Fig. 2. There is no high resolution optical image to associate the two peaks with equivalent features in the optical. We will use the eastern, lower peak as the center of our azimuthal profiles since it appears to better represent the centroid of the diffuse emission from RR 22.

To measure the extent of the sources associated with the pairs, we have produced surface brightness profiles of the emission centered on the brighter object (when both are detected) and azimuthally averaged. A circle of $r = 0.'2$ centered either on unrelated sources (∼2′ to the SE in RR 22 and to the N in RR 216), or on the fainter galaxy (RR 210) has been masked out. In RR 143, the angular sector between −10° and +80° is masked out in the 0.′6−1′ region, to avoid the possible contribution from a background source. In RR 259, the profile is azimuthally averaged except in the 0.′5−2′ region, where the SW quadrant (180°−270°) is excluded from the data to avoid the emission from RR 259a.

3.1. Extent of the sources

Figure 4 shows the comparison between the radial profile of the net emission from the galaxies and the Point Spread Function (PSF), assumed at the field's center and arbitrarily normalized to the data to match the innermost point. In all cases, the emission is more extended than the PSF. The outermost radius ranges from ∼0.′5 (RR 210a) to ∼7′ (RR 143), and from ∼5 (RR 210a) to ∼182 kpc (RR 22) in linear scale (see Table 3). The data for RR 210b (NGC 4106) and RR 259a are of too poor quality for a meaningful assessment of the extent.

Several sources appear to be extended on scales much larger than galactic (cf. a_{25} or R_{90} in Table 2). A parameterization with a "King-type" profile, $\Sigma_x \propto (1 + (\frac{r}{r_c})^2)^{-3\beta+0.5}$, is reasonable, and gives core radii of a few arcsec (from 2″ to 6″), corresponding to 1–3 kpc on a linear scale. These core radii are similar to those found in other galaxies observed at high resolution (Trinchieri et al. 1986; Irwin & Sarazin 1996; Dahlem & Stuhrmann 1998).

Although a single function can parameterize the profiles of these objects to first approximation, in a few cases the fit is not as good as in other cases (see Fig. 5). A clear excess is seen in the profile of RR 242 at $r \sim 3'-5'$.

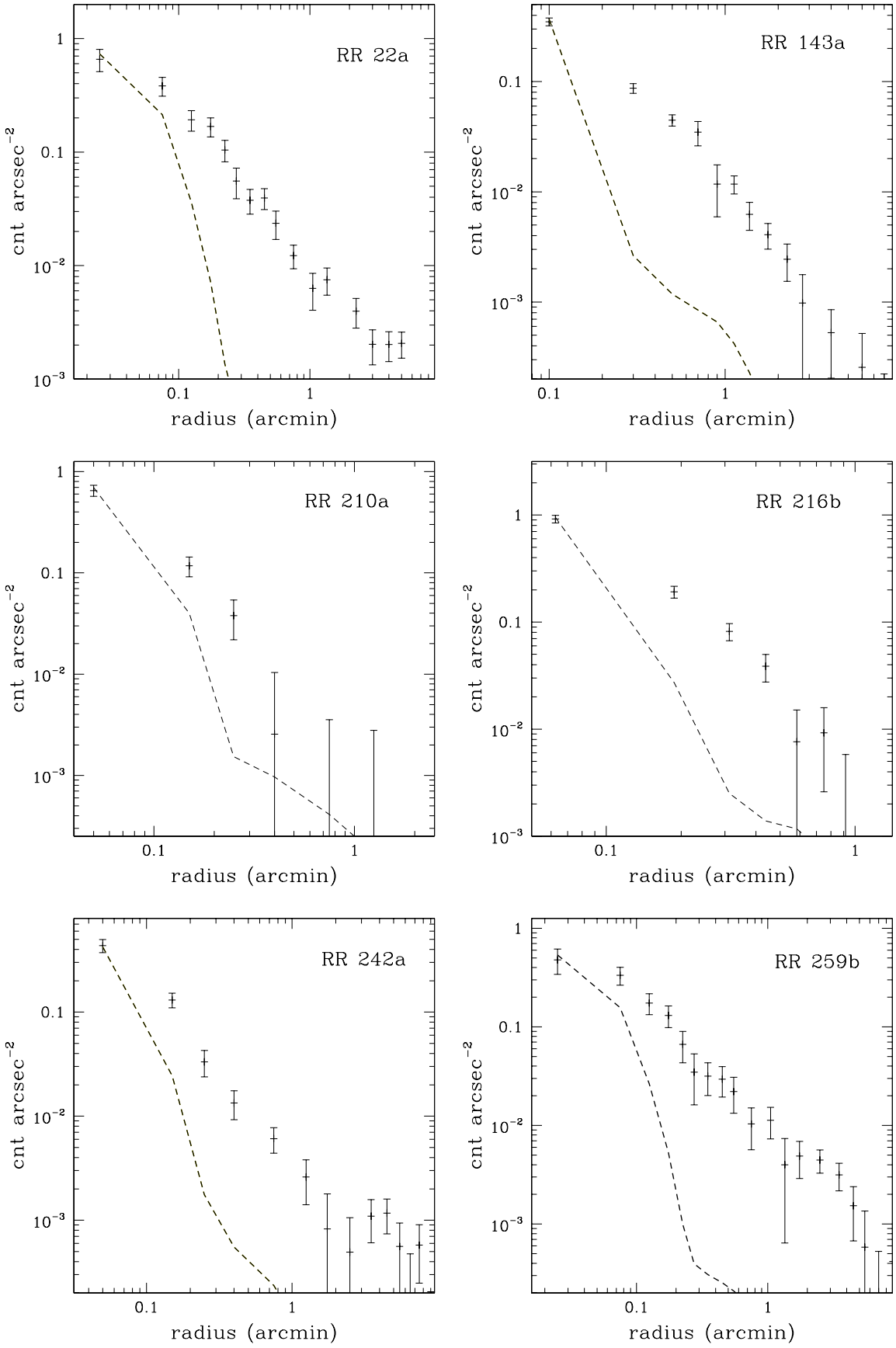

Fig. 4. Radial profile of the net emission from the detected objects. Data are azimuthally averaged in concentric annuli about the X–ray peak. The dashed line represents the ROSAT-HRI PSF at the field's center arbitrarily normalized to the central bin.

The statistics are not sufficient to properly locate these excess photons in different quadrants, also considering the non-uniformity of the HRI background due to different gain values across the detector (see above). However, it appears that a separate low surface brightness source could be present in the S-SW quadrant, though without any optical counterpart either from NED or from the visual inspection of the DSS frame. We will conservatively assume that the excess is not related to RR 242, and defer the proper understanding of this excess to future, deeper X–ray observations of the field. However, we cannot exclude an association with RR 242 at this stage (see discussion and Miller et al. 1999).

A hint of a flattening is visible in RR 22, at a radius of $\sim 3'$. Radial profiles of X–ray bright poor groups often require two components, a smaller one related to the central galaxy, and a more extended one, related to the group emission (MZ98, Helsdon & Ponman 2000). Given the optical similarity of RR 22 with the sample in MZ98, we could expect a second component to accommodate both the galaxy and the group contribution. With the higher spatial resolution of the HRI, however, the galaxy component has $r_c(1)$ is <3 kpc, much smaller than the typical values found by MZ98 (however, see Helsdon & Ponman 2000).

3.2. Fluxes and luminosities of the sources

Although in some cases the X–ray emission is much more extended than expected from the optical size, the emission is typically associated with the early-type member of the pair. In RR 259 the two sources appear to blend into one another. However, even in this case, they appear like two separate peaks associated with the two galaxies. We have derived the flux of the sources detected from the net counts within the maximum source extent, and converted assuming a 1 keV *raymond* spectrum with 100% cosmic abundances and line-of-sight column density (Dickey & Lockman 1990). For RR 210b (NGC 4106) and RR 259a we have assumed a circle of $18''$ appropriate for a point source at the field's center, to obtain fluxes for these sources. The resulting fluxes and luminosities are summarized in Table 3, for each detected object.

4. Discussion and conclusions

All pairs studied here have at least one detected member, and in all cases the brightest, early type member of the system is associated with the stronger X–ray source. The radial surface brightness profiles are inconsistent with the instrument response, indicating X–ray sources with different angular (and linear) extent: from RR 210b ($0\farcm3$, or 3 kpc) to RR 22a ($5\farcm5$, or 182 kpc).

As shown by Fig. 6, in spite of the very small number of objects presented here, the distribution of L_X and L_x/L_b spans the whole range of X–ray luminosities of early type galaxies. We also include the data for RR 75 (NGC 1316/1317), which is entirely consistent with the rest of the sample. This indicates that there is no evidence in our data that the physical state of pairs influences their X–ray properties, at least to the first order. Interactions, merging or tidal forces that are expected from their relative proximity and are observed in their optical morphology or dynamics (see Sect. 2) do not appear to significantly modify the overall level of X–ray emission nor their gross morphological appearance. None of the pairs presented here has an X–ray morphology similar to that of the spectacular NGC 4782/4783 system, a colliding elliptical galaxy pair, where high resolution X–ray observations reveal a complex distribution of the hot gas around the two galaxies, including an X–ray bridge connecting the two, tidal tails and gas at the interaction interface (Colina & Borne 1995). On the other hand, even in this pair, L_X does not appear significantly enhanced relative to other galaxies (Fig. 6). This is consistent with the discussion in Read & Ponman (1998), who find that the X–ray luminosity should not be strongly affected by the interaction/merging processes, at least not as much as the emission at other wavelengths (e.g. far-infrared). We could expect smaller perturbations in the hot gas distribution, as a consequence of the dynamics in the pairs studied, but we might not have the sensitivity to see them, or they might require peculiar conditions to be seen in X–rays and/or might be rare phenomena not covered by the small sample tested here.

We cannot even interpret the large spread in X–ray luminosity as evidence of different stages in the interaction/merging process. At least three of the pairs studied here display clear evidence of ongoing/strong interaction. The line strength indices in RR 210 (Longhetti et al. 2000), and the distortion induced by RR 216a in the companion disk galaxy RR 216b, that are much more prominent than those associated with the early type member (R&R96), testify to the strong on-going interactions in these two pairs (see Sect. 2). In RR 259, several studies in different bands indicate that this system suffered recent strong interactions which are still going on (see e.g. Duc & Mirabel 1998). Large amounts of cold gas are present and the long tails, produced by the interaction, are indicated as the birthplace of tidal dwarf galaxies. Duc & Mirabel suggest that RR 259b (NGC 5291) could even be the result of a complete merger between gas rich spirals. This galaxy is also strongly interacting with the nearby companion now. In this sense, NGC 5291 is the only galaxy among the pairs in our present sample that could be considered close to the final steps in the "merging sequence" of Toomre, whose X–ray properties have been studied by Read & Ponman (1998). If so, RR 259b is relatively "young" in terms of total merger lifetime, still has a few Gyr of evolution to go through before it will resemble a more "typical" elliptical. The features shown by all three place the pairs at the beginning of an interacting sequence (see Noguchi 1990). And yet, the L_X/L_B in these three pairs is significantly different: while RR 259 is at the bright extreme of the distribution, RR 210 is at the opposite end, with RR 216 somewhere in the middle.

Table 3. Basic X–ray properties.

pair member	extension (arcmin)	extension (kpc)	counts	count rate	flux (0.1–2 keV)	log L_X (erg s^{-1})	log L_B $L_\odot$	log L_X/L_B
RR 22a	5.5	182	1143 ± 151	0.05	1.7×10^{-12}	42.43	11.36	31.06
RR 143a	7.0	165	1008 ± 173	0.04	2.2×10^{-12}	42.45	10.88	31.57
RR 210a	0.5	5	140 ± 22	0.0017	6.0×10^{-14}	40.06	10.86	29.20
RR 210b	—	—	54 ± 14	0.0007	2.0×10^{-14}	39.58	10.75	28.83
RR 216b	0.83	16	430 ± 38	0.005	1.8×10^{-13}	41.00	10.65	30.34
RR 242a	3.0	60	270 ± 50	0.018	7.2×10^{-13}	41.62	10.84	30.78
RR 259a	—	—	41 ± 13	0.0007	2.6×10^{-14}	40.38		
RR 259b	6.0	127	1028 ± 357	0.018	6.5×10^{-13}	41.76	10.44	31.32

Notes: The fluxes are derived from the net counts, assuming a 1 keV *raymond* spectrum with line-of-sight Galactic N_H. Net counts are derived within the maximum extension listed in the table, above the field background (see text).

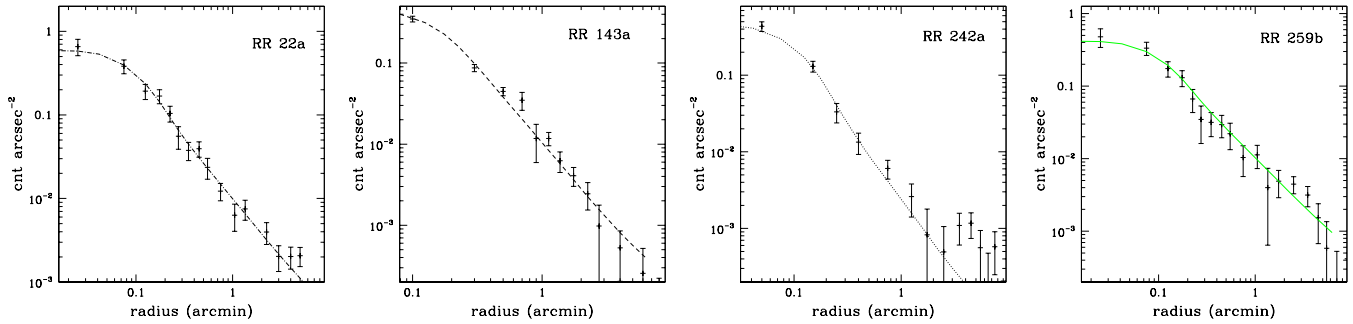

Fig. 5. Surface brightness profiles of the extended objects compared to King-type laws (solid lines). The core radii of the King law applied are in the range $0\farcs5 \leq r_c \leq 6\farcs$ while β ranges between 0.4 and 0.5.

Further support comes from the data presented by Henriksen & Cousineau (1999), who have selected an equivalent set of pairs in the northern hemisphere. They have analyzed a much larger sample of objects, but they have obtained a similar number of "detections" for the early type or mixed morphology type objects. We have added their data in Fig. 6. We have not included CPG 236, CPG 235 and CPG 510, since they all include a Seyfert galaxy, and their X–ray emission is dominated by the AGN. We have also plotted the detections with two different symbols. Filled symbols refer to the detection of the "single" galaxy in the pair (as shown by their Fig. 19, emission from CPG 278 is almost equally divided between the two members, and the X–ray source associated with CPG 353 coincides only with the early type member, their Fig. 20; notice that this is NGC 4649, a well studied galaxy in the Virgo cluster, see e.g. Trinchieri et al. 1997a, 1997b). Open circles instead are used for CPG99 and CPG584, for which the X–ray source is associated with both members, and for CPG 278 (a detection is given in their Table 3, but no additional information nor figures are given). Upper limits are also given, associated with the whole pair. In all cases, detections are fully consistent with the sample of normal galaxies.

If interpreted as a tracer of the potential well, diffuse X–ray emission could be used to better understand the dynamical evolution of a "pair". As remarked in Sect. 2, all pairs except RR 22 show signatures that characterize interacting systems. However, from the optical data we have little information on whether they are bound system, or whether they are first time, unbound encounters. RR 22 is the only system that appears to be bound, although it might not be a "true pair", since it is the dominant pair in a poor group of satellite galaxies with a velocity dispersion of ≈300 km s^{-1}.

From the X–ray picture, we could expect deep potentials associated with other objects in the sample, like RR 143, RR 259 and possibly RR 242. RR 143, optically similar to RR 22, represents somewhat of a puzzle. It appears isolated in space, but the X–ray luminosity and extent, reminiscent of poor groups, suggests instead a relative deep potential. The apparent isolation could reflect the lack of deep observations that would reveal a large population of much fainter galaxies, as optical observations by Zabludoff & Mulchaey (1998) have shown. The high velocity separation between the two members and the relatively weak evidence of interaction could be indicative that they form an optical alignment, although a high velocity encounter cannot be excluded.

The extension of the gas in RR 259 is also quite large, and could signify that both galaxies are bound in a common potential.

RR 242, a very isolated system on the DSS frame, is a more ambiguous case. We have conservatively discarded

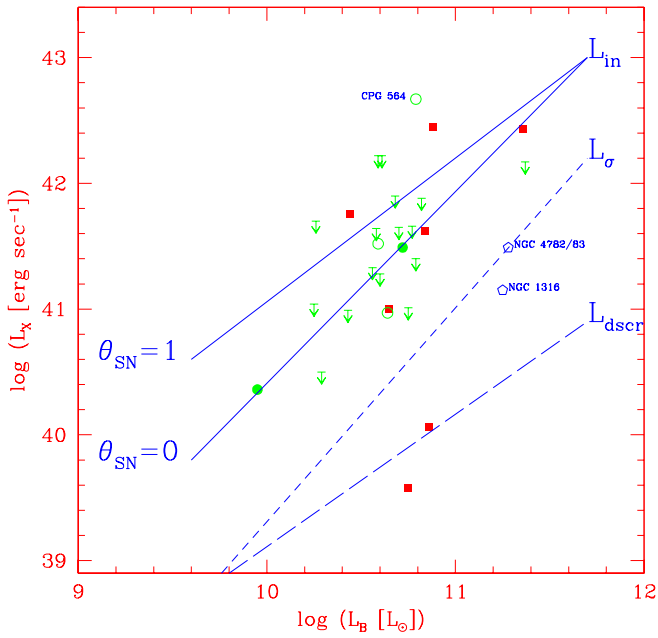

Fig. 6. Galaxies in the present sample (squares) and those in the HC99 sample of E+E and E+S pairs (dots and upper limits). Data for NGC 4782/83 are from Colina & Borne (1995) and NGC 1316 from Beuing et al. (1999; see also Kim et al. 1998). The lines shown give an indication of the full range of X–ray luminosity of the "normal" galaxies e.g. in the sample of Beuing et al. (1999), which is not plotted here for clarity. Solid lines ($L_{\rm in}$) represent the expected X–ray luminosity of steady-state cooling flow model for different supernova rates; the dashed line indicates the heating due to stellar motion (L_σ); the long dashed line ($L_{\rm dscr}$) represents the expected contribution from discrete stellar X–ray sources. Models are from Ciotti et al. (1991).

the possibility that the observed extension is related to the galaxy, given the limited quality of the observation. However, Miller et al. (1999) report a detection from the ROSAT All-Sky Survey which indicates that the X–ray source has an estimated extension of 195 kpc. Deeper X–ray observation and, in particular, deeper optical observation are needed to investigate the environmental characteristics of this pair (e.g. dwarf galaxy population and its velocity distribution). Nevertheless, though not as extreme as RR 22 or RR 143, the X–ray luminosity is consistent with a significant fraction of hot gas in this system as well.

RR 210 and RR 216, instead, don't show evidence of a deep potential associated with them. Their X–ray emission is consistent with the lowest X–ray-to-optical luminosity ratio objects, for which the dominant emitting component is the evolved stellar population. A similar case was presented in Rampazzo et al. (1998): CPG 416 (NGC 5480/NGC 5481), an almost twin sister to the NGC 2300 group, also showed no evidence of the extended X–ray emission displayed by the latter system, and was interpreted in the framework of unbound encounters. The more sensitive observations of these two systems have allowed us to detect the galaxies, but have given no indication of extended, high luminosity emission. Since these happen to be the closest systems among the ones we have studied here, and have the most sensitive observations, we can discard the possibility that we have missed it due to limits in the sensitivity, and we can therefore be reasonably sure that their X–ray characteristics are dissimilar to those of RR 143 or RR 259.

Acknowledgements. We thank Anna Wolter for the use of her best fitting package. This work has received partial financial support from the Italian Space Agency. GT thanks Prof. Trümper and the MPE for hospitality while part of this work was done. This research has made use of the NASA/IPAC Extragalactic Database (NED) which is operated by the Jet Propulsion Laboratory, California Institute of Technology, under contract with the National Aeronautics and Space Administration, and of the ROSAT Data Archive of the Max-Planck-Institut für extraterrestrische Physik (MPE) at Garching, Germany.

References

Arp, H. C., & Madore, B. F. 1987, Catalogue of Southern Peculiar Galaxies and Associations, vols. 1, 2 (Cambridge: University Press)
Beuing, J., Döbereiner, S., Böhringer, H., & Bender, R. 1999, MNRAS, 209, 221
Cappi, A., Da Costa, L. N., Benoist, C., Maurogordato, S., & Pellegrini, P. S. 1998, AJ, 115, 2250
Carollo, C. M., Danziger, I. J., & Buson, L. 1993, MNRAS, 265, 553
Carollo, C. M., & Danziger, I. J. 1994, MNRAS, 270, 523
Ciotti, L., Pellegrini, S., Renzini, A., & D'Ercole, A. 1991, ApJ, 376, 380
Colina, L., & Borne, K. D. 1995, ApJ, 454, L101
Combes, F., Rampazzo, R., Bonfanti, P., Prugniel, Ph., & Sulentic, J. W. 1995, A&A, 297, 37
Dahlem, M., & Stuhrmann, I. 1998, AA, 332, 449
Dickens, R. J., Currie, M. J., & Lucey, J. R. 1986, MNRAS, 220, 679
Dickey, J. M., & Lockman, F. J. 1990, ARA&A, 28, 215
Duc, P.-A., & Mirabel, I. F. 1998, A&A, 333, 813
Elmegreen, D. M., & Elmegreen, B. G. 1982, MNRAS, 201, 1021
Fabbiano, G., Schweizer, F., & Mackie, G. 1997, ApJ, 478, 542
Garcia, A. M. 1993, A&AS, 100, 47
Henriksen, M., & Cousineau, S. 1999, ApJ, 511, 595
Helsdon, S. F., & Ponman, T. J. 2000, MNRAS, 315, 356
Karachentsev, I. D. 1987, Dvoinye Galaktiki (Nauka, Moskow)
Kim, D.-W., Fabbiano, G., & Mackie, G. 1998, ApJ, 497, 699
Knapp, G. R., Guhathakurta, P., Kim, D.-W., & Jura, M. 1989, ApJS, 70, 329
Irwin, J., & Sarazin, C. 1996, ApJ, 471, 683
Lauberts, A., & Valentijn, E. A. 1989, The Surface Photometry Catalogue of the ESO-Uppsala Galaxies, ESO: ESO-LV
Lloyd, B. D., Jones, P. A., & Haynes, R. F. 1996, MNRAS, 279, 1187
Longhetti, M., Rampazzo, R., Bressan, A., & Chiosi, C. 1998, A&AS, 130, 267
Longhetti, M., Bressan, A., Chiosi, C., & Rampazzo, R. 2000, A&A, 353, 917
Maia, M. A. G., da Costa, L. N., & Latham, D. W. 1989, ApJS, 69, 809

Miller, N. A., et al. 1999, ApJ, 118, 1988
Mulchaey, J. S., Davis, D. S., Mushotzky, R. F., & Burstein, D. 1993, ApJ, 404, L9
Mulchaey, J. S., Davis, D. S., Mushotzky, R. F., & Burstein, D. 1996, ApJ, 456, 80
Mulchaey, J. S., & Zabludoff, A. I. 1998, ApJ, 496, 73
Mulchaey, J. S., & Zabludoff, A. I. 1999, ApJ, 514, 133
Noguchi, M. 1990, Dynamics and Interaction of Galaxies, ed. R. Wielen (Springer-Verlag), 469
Pildis, R., Bregman, J. N., & Evrard, A. E. 1995, ApJ, 443, 514
Ponman, T. J., Bourner, P. D. J., Ebeling, H., & Böringer, H. 1996, MNRAS, 283, 690
Ramella, M., Focardi, P., & Geller, M. J. 1996, A&A, 312, 745
Rampazzo, R., & Sulentic, J. W. 1992, A&A, 259, 43
Rampazzo, R., Covino, S., Trinchieri, G., & Reduzzi, L. 1998, A&A, 330, 423
Reduzzi, L., & Rampazzo, R. 1995, Astr. Lett. Comm., 30 Nos. 1–6 (Gordon & Breach), 1: R&R95
Reduzzi, L., & Rampazzo, R. 1996, A&AS, 116, 515: R&R96
Rose, J. A. 1984, AJ, 89, 1238
Rose, J. A. 1985, AJ, 90, 1927
Sadler, E. M., & Sharp, N. A. 1984, A&A, 133, 216
Sulentic, J. W., Pietsch, W., & Arp, H. 1995, A&A, 298, 420
Trinchieri, G., Fabbiano, G., & Canizares, C. 1986, ApJ, 310, 637
Trinchieri, G., & Pietsch, W. 2000, A&A, 353, 487
Trümper, J. 1983. Adv. Space Res., 2(4), 241
Trümper, J., Hasinger, G., Aschenbach, B., et al. 1991, Nature, 349, 579
Tully, B. R. 1988, Nearby Galaxy Catalogue (Cambridge University Press)
Zabludoff, A. 1999, The Stellar Content of Local Group Galaxies, IAU Symp. 192, ed. P. Whitelock, & R. Cannon, in press
Zabludoff, A. I., & Mulchaey, J. S. 1998, ApJ, 496, 73
Zombeck, M. V., David, L., Harnden, F. R., & Kearns, K. 1995, Proc. SPIE, 2518, 304